frontiers | Frontiers in Earth Science

TYPE Original Research
PUBLISHED 24 January 2023
DOI 10.3389/feart.2022.1039487

OPEN ACCESS

EDITED BY
Zizheng Guo,
Hebei University of Technology, China

REVIEWED BY
Payam Tehrani,
Amirkabir University of Technology, Iran
Chaoxuan Zhang,
Institute of Rock and Soil Mechanics (CAS), China
Rulong Bn,
Guilin University of Technology, China

*CORRESPONDENCE
Dewen Liu,
civil_liudewen@sina.com

SPECIALTY SECTION
This article was submitted to Geohazards and Georisks, a section of the journal Frontiers in Earth Science

RECEIVED 08 September 2022
ACCEPTED 14 December 2022
PUBLISHED 24 January 2023

CITATION
Chen L, Wang T, Wang Q, Liu D, Xiao Z, Liao G, Yang Z and Lei M (2023), Study on failure modes of a new staggered story isolated structure based on IDA method.
Front. Earth Sci. 10:1039487.
doi: 10.3389/feart.2022.1039487

Study on failure modes of a new staggered story isolated structure based on IDA method

Lihao Chen[1], Taize Wang[1], Qinyue Wang[1], Dewen Liu[1]*, Zhiyi Xiao[1], Gengjie Liao[1], Zhuoxin Yang[1] and Min Lei[2]

[1]School of civil engineering, Southwest Forestry University, Kunming, China, [2]School of civil engineering, Southwest Jiaotong University, Chengdu, China

New staggered story isolated structure is a new type of isolated system. This paper explores the failure mode of a new staggered story isolated structure with the increment dynamic analysis (IDA) method. On the basis of a finite model of a new isolated structure with staggered stories, a failure criterion for isolated structure was established. The findings indicate that the new staggered, isolated structure has good collapse resistance. When the story angle limit is 1/100, the primary structure will fail before the isolated layer in the event of a strong earthquake, and failure typically happens at the base of the structure where components with a higher bearing capacity should be used. Under the impact of the P-δ effect, the upper isolated layer is more prone to failure than the lower isolated layer. The upper isolated layer may have a tensile stress exceeding 1MP and a horizontal displacement exceeding 385 mm, which may lead to the risk of structural overturning. Therefore, higher strength supports should be selected for the weak position of the isolated layer.

KEYWORDS

isolated structure, failure criterion, failure mode, IDA, failure path

1 Introduction

The new staggered story isolated structure is a type of multi-layer isolated structure derived from the foundation isolated structure and the inter-story isolated structure. The study found that, compared with general seismic structures, when a high-rise building is equipped with a seismic isolated layer, the upper structure above the seismic isolated layer has high seismic resistance as a seismic isolation structure, which can greatly reduce the risk of physical damage to the building(Sueoka et al., 2004; Tsuneki et al., 2008; Becker et al., 2015). The traditional isolated structure designates a particular layer as the isolated layer, while the new staggered story isolated structure distributes the isolated layer in different layers of the structure. The new staggered story isolated system is applicable to the frame-core tube structure, and its most notable feature is to ensure the coherence of the core tube part. The isolated bearings of the new staggered story isolated structure are not arranged on the entire isolated layer but staggered in two isolated layers with different heights. The base isolated layer of the core tube is positioned at the base of the structure, while the upper isolated layer of the frame is located in the middle of the primary

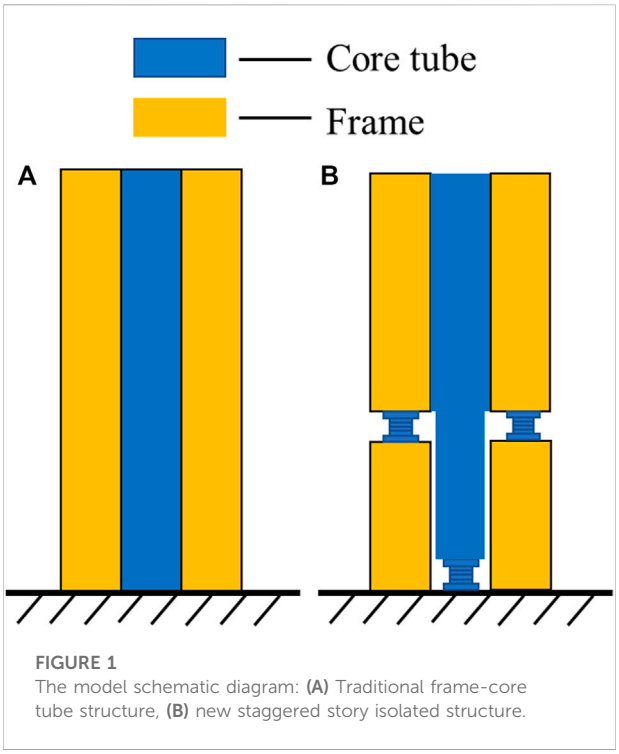

FIGURE 1
The model schematic diagram: **(A)** Traditional frame-core tube structure, **(B)** new staggered story isolated structure.

structure. Figure 1 shows the model schematic diagram of the traditional frame-core tube structure and the new staggered story isolated structure.

Currently, the isolated system has been widely used in engineering (Kelly, 1990; Faiella and Mele, 2020) and unique architectural structures (Whittaker et al., 2018; Zhou et al., 2018). It is proved that the isolated structure has a good aseismic performance by comparing the structural response of the isolated structure and aseismic structure under ground motions (Pant and Wijeyewickrema, 2012; Tavakoli et al., 2015). Several scholars have compared the structural responses of different types of seismic isolators under ground motions and discovered that different types of isolators have distinct control effects on seismic responses (Derham et al., 1985; Castaldo and Tubaldi, 2018; Shan et al., 2020). Taha Nazarnezhad et al. (Nazarnezhad and Naderpour, 2021) focused on the vulnerability of base isolated structures under near-fault ground motion and found that structural damage was induced mostly by excessive floor acceleration. Ye et al. (2009) optimized the Calvin model to simulate the collision behavior of the base-isolated structure under near-fault ground motion and discovered that the excessive flexibility of the isolation system may result in the base-isolated structure. Zhuang et al. (Haiyang et al., 2014) evaluated the seismic response of the isolated structure considering the SSI effect through a shaking table test and found that the SSI effect would diminish the isolated efficiency of the isolated layer. Kim et al. (2018); Kim and Kang, (2018) investigated the isolated performance control of high-rise inter-story isolated structures. Several optimization methods have been proposed to evaluate the structural response of isolated structures subjected to the combined effects of ground motion and wind (Wang et al., 2012; Loh et al., 2013; Zhao et al., 2019). Zhou et al. (2016) proposed a simplified model that can be utilized for inter-story isolated structures and analyzed the influence of the isolated layer on the reduced structural response at various heights, revealing that the lower the isolated layer, the greater the effect. Chang et al. (Chang and Zhu, 2011) obtained the vulnerability curve of the inter-story isolated structure using dynamic inelastic time-history analysis with random samples, and the analysis demonstrated that the inter-story isolated structure possessed superior response characteristics than the RC structure. Liu et al. (2022); Zhang et al., (2022) compared the new staggered story isolated structure with the traditional seismic isolated structures and found that its seismic performance is better than that of the inter-story isolated structure and that the structural stiffness is reduced when considering the SSI effect.

The partial or weak layer failure mode typically causes structural collapse, which leads to the failure of the anti-collapse performance of the structure to fully play, rendering it unable of effectively resisting the impact of earthquakes or other effects. Therefore, it is crucial to identify the failure modes of structural systems, control and reinforce them (Song et al., 2017). Failure modes of structures are mostly addressed using dynamic incremental analysis (IDA) as a subfield of reliability theory (Zhou et al., 2013; Yan and Xu, 2018; Güneş and Ulucan, 2021; Pan et al., 2021). Shoma Kitayama et al. (Kitayama and Constantinou, 2019) employed Push over method to determine the collapse resistance of isolated structures. Through the study of different structural models, it is found that compared with the traditional push over method, the IDA method has higher accuracy in evaluating the seismic demand and capacity of the structure(Navideh et al., 2012; Ahmadi et al., 2020; Shafigh et al., 2021). On the basis of the IDA method, a vulnerability assessment of super high-rise structures is conducted, and a combined control scheme is developed to control the structural inter-story displacement (Zheng et al., 2015; He and Lu, 2019). For the isolated structure, it has been determined that the failure of the structure typically happens in the isolated layer (Zhang et al., 2018; Shi and Du, 2021) or weak spots of structures below the isolated layer (Tan et al., 2020). Liu et al. (Jin et al., 2020) calculated and analyzed the dynamic reliability of the inter-story isolation system to determine the total failure probability of the structure. Du Yongfeng et al. (Du et al., 2018) utilized the non-linear Pushdown analysis method to study the vertical continuous collapse mechanism of the base isolated structure. They compared the failure rates of the isolated layer and the

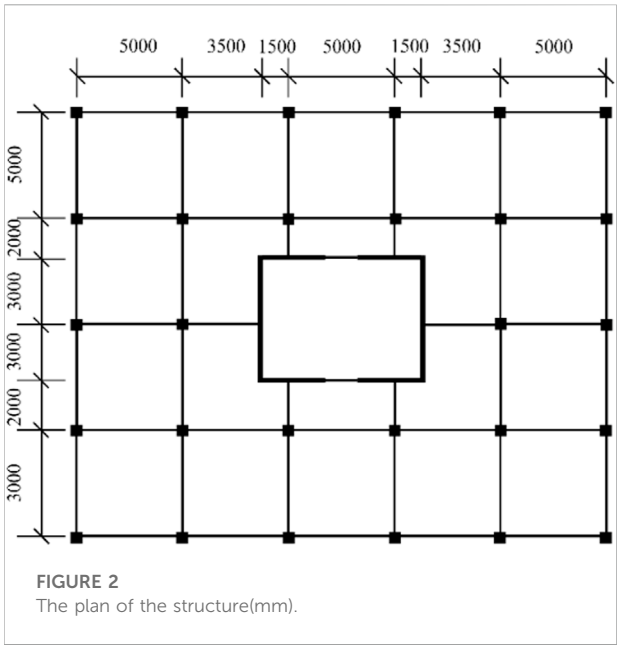

FIGURE 2
The plan of the structure(mm).

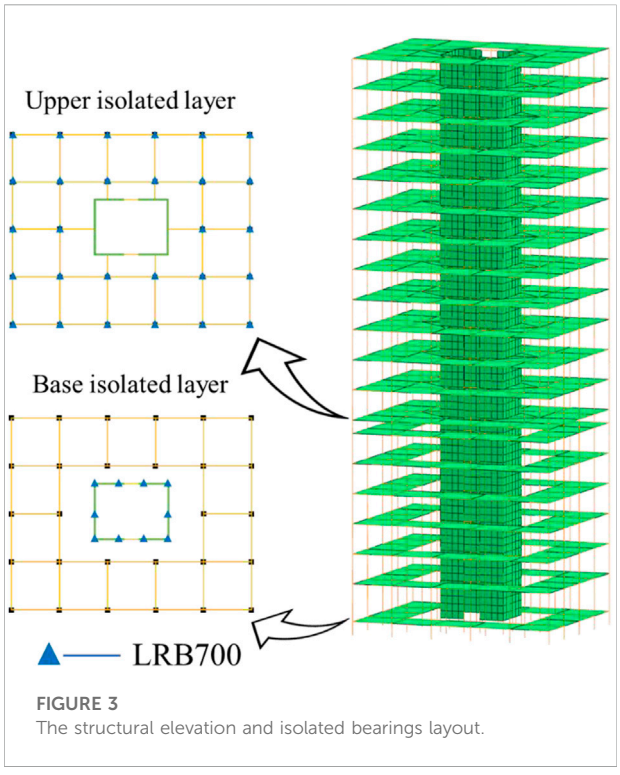

FIGURE 3
The structural elevation and isolated bearings layout.

superstructure and discovered that the isolated layer was more prone to failure. Castaldo et al. (2015) proposed a method for evaluating the reliability of base isolated structures based on single/bidirectional displacement limit states. Tan et al. (2017) studied the failure modes of isolated continuous girder bridges subjected to strong ground motion by using the weighted rank sum ratio method combined with the established three-dimensional finite element bridge model. For the failure mode optimization scheme of wood structures, it was determined that the material properties of wood (Franke et al., 2015) and structural stress (Huan et al., 2018) should be taken into consideration.

Scholars have extensively employed the IDA approach to analyze the failure modes of various structures systematically, but there is no relevant research on the failure modes of new staggered story isolated structures. The ground motions with different spectral characteristics will induce the dispersion of IDA analysis results. Therefore, ten ground motions that are in good agreement with the response spectrum of the seismic specification are selected to limit the difference in the study results. After determining the failure mode of the new staggered story isolated structure, the weakest failure mode of the new staggered story isolated structure is optimized by reinforcing the isolated layer and weak components to enhance the seismic performance of the new staggered story isolated structure. The conclusions of the study will provide an urgent theoretical basis for seismic isolation design in areas with potential earthquake hazards and promote the development of seismic isolation design methods and the improvement of seismic isolation measures for high-rise building structures.

2 Model of new staggered story isolated structure

2.1 Structural design

The model structure under investigation is an 18-story frame-core tube structure. According to the requirements of Code for Seismic Design of Buildings (Ministry of Housing and Urban-Rural Development (2010), Code for Design of Concrete Structures (Ministry of Housing and Urban-Rural Development (2010), and Technical Specification for Concrete Structures of Tall Buildings (Ministry of Housing and Urban-Rural Development (2010), YJK is used for seismic structure design. Seismic fortification intensity of 8° (.2 g). The base isolated layer is positioned at the bottom of the core tube, while the upper isolated layer is positioned in the seventh layer of the structure. The height of the isolated layer is 1.6 m. The concrete grade of the beam, column, plate, and shear wall is C40, and the protective thickness of beam and column is 20 mm. The plan of the structure is depicted in Figure 2.

The column section size is 800 mm × 800 mm in 1–10 layers, 700 mm × 700 mm in 10–18 layers, the beam section size is 750 mm × 350 mm, the connecting beam is 700 mm × 350 mm, and the thickness of the shear wall of the core tube is 250 mm. After seismic isolated design, the major structure according to 7° (0.15 g) seismic isolated fortification reinforcement design and the longitudinal reinforcement and stirrup of the beam, column, and shear wall is HRB400, the rest of the reinforcement using

TABLE 1 Parameters of lead-rubber isolated bearings.

Type	Effective diameter D_E/mm	Vertical stiffness KE/kN·m^{-1}	Stiffness before yield K/kN·m^{-1}	Stiffness ratio after yield KYR	Yield force KY/kN	Total thickness of rubber T_r/mm
LRB700	700	1.894e + 006	13,456	0.077	116.8	140

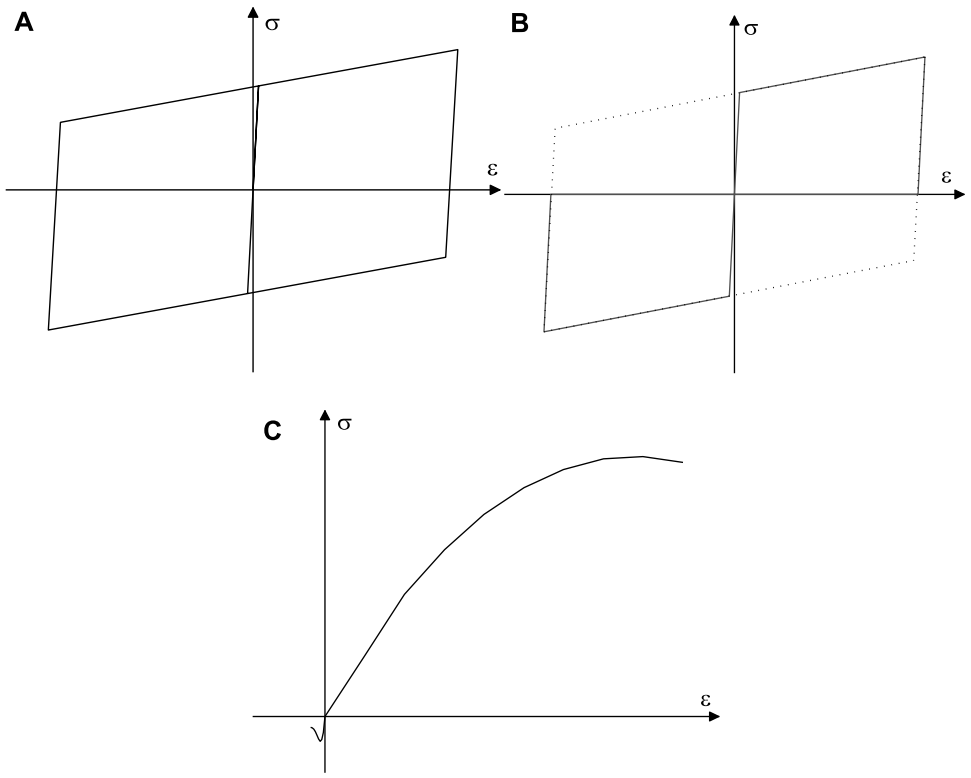

FIGURE 4
Material models: **(A)** Reinforcement, **(B)** Isolated bearings, **(C)** Concrete.

HPB300. Figure 3 depicts the structural model elevation and isolated bearing layout strategy.

2.2 Structural modelling

Structural failure is a highly complex dynamic response process due to the presence of many strong non-linear factors. The softening effect of concrete is the primary cause of structural failure and even collapse. The elastoplastic damage constitutive model of concrete is found to be superior at capturing the complex post-negative peak behavior of concrete. In this paper, a double scalar elastoplastic damage constitutive model of concrete is used to simulate and express the failure modes of structures subjected to ground motion, and the expressions are as follows:

$$\sigma = (\mathrm{I} - \mathrm{D}) : C_0 : \left(\varepsilon - \varepsilon_p\right) \tag{1}$$

where σ and ε are stress and strain, respectively; C_0 is the initial elastic stiffness tensor; I is the unit tensor; ε_p is the plastic strain tensor; D is the damage tensor and can be decomposed into

$$\mathrm{D} = d^{+}\mathrm{P}^{+} + d^{-}\mathrm{P}^{-} \tag{2}$$

where d^{+} and d^{-} are the damage variables under tension and compression, respectively; P^{+} and P^{-} are the projection tensors of the damage variables, which are obtained from the effective stress through spectral decomposition.

Parameters of lead-rubber isolated bearings are listed in Table 1. LRB700 bearings are selected for the structure and arranged at the base of the core tube and the seventh layer of the frame, respectively. The seismic isolated bearing meets the

TABLE 2 Structural Modal periods and modal participation factors.

Mode no.	Period/s	Participation factors		
		X-Component	Y- Component	Z- Component
1	2.204	−11.900	−3116.9	−2.6982
2	2.184	3112.0	−11.961	1.0538
3	1.835	23.044	13.608	−0.17314
4	0.587	861.00	−6.7627	−4.0812
5	0.581	−6.6086	−890.15	14.256
6	0.459	0.42176	16.871	1.8993

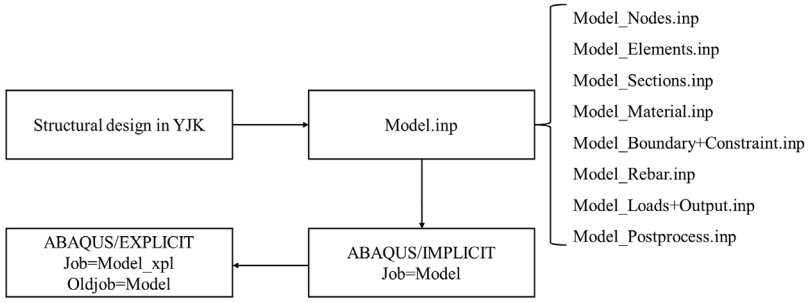

FIGURE 5
Behavioral model.

design standard that the compressive stress of the structure under gravity load is less than 15 MPa. The ratio of the average response spectrum value of the ground motion combination to the standard response spectrum value in the first-order period is considered to be between 0.8 and 1.2. Abaqus was utilized for the non-linear analysis of the structure, fiber beam elements were utilized for the beam and column, layered shell elements were utilized for the shear wall, and Connector elements were utilized for vibration isolated bearings. The constitutive model of concrete, reinforcement and isolated bearings are shown in Figure 4. Linear dynamic analysis is performed on the structural model established in ABAQUS, and the structural modal periods and modal participation factors are obtained, as shown in Table 2.

The behavioral model in Figure 5 clarifies the design process. By reading the structural model file in YJK, a three-dimensional geometric model of the structure is generated (Model_Nodes.inp, Model_Elements.inp). Then read the design result file to record the component section, material and reinforcement information, and finally output the inp model data file (Model_Sections.inp, Model_Material.inp, Model_Boundary.inp et al.) that can be read by ABAQUS through model processing. The generated model is solved by implicit algorithm and explicit algorithm in two steps in ABAQUS. The first step is to submit the Model.inp to the ABAQUS/IMPLICIT module for static analysis under the action of gravity. The second step is to read the new model file generated by the calculation results of the first step and submit the Model_xpl.inp for dynamic analysis under the action of ground motion in the ABAQUS/EXPLICIT module.

3 Failure criterion

3.1 Failure criterion of isolated layer

The failure criteria of an isolated layer are the horizontal shear deformation and vertical stress limits specified in the Code for Seismic Design of Buildings (GB 50011-2010).

1) When the horizontal displacement of the isolated layer surpasses the lesser of 0.55 times the effective diameter of the smallest bearing in the isolated layer and 3 times the entire thickness of the rubber, the isolated layer fails.

The horizontal displacement failure threshold of LRB700 isolated layer is obtained

$$L_{\max} = \max[0.55D_b, 3T_r] = 385 \text{ mm} \quad (3)$$

TABLE 3 Limit state of story drift at different performance levels.

Quantitative index	Seismic performance level				
	Normal use	Basic use	Repair use	Life use	Near Collapse
Interstorey drift	1/800	1/400	1/200	1/100	1/50

2) When the compressive stress of the isolated layer surpasses 30 MPa, which is considered the failure of the isolated layer, the vertical stress of the rubber isolated bearing exceeds the limit. Considering the internal damage of rubber under tension and the overturning risk of the major structure following the tensile stress of the isolated bearing, the tensile stress of the isolated bearing should not exceed 1 MPa.

3.2 Failure criterion of major structure

In structural design, the limit value of the story drift must be addressed to avoid excessive story drift of the building structure and additional bending moment that will lead to the collapse of the structure. The structure is allowed to exhibit apparent non-structural displacement, but the displacement value must be controlled within a safe range in the normal limit state of the building. By controlling the limit value of the story drift, the effect of external impact force on the stiffness of high-rise buildings can be effectively avoided. The failure of the structure is triggered by the gradual accumulation of member failures. For the reinforced concrete members, displacement angle between structure layers can be utilized as an evaluating criterion. When the story drift of the major structure reaches the elastic-plastic story drift limit, the major structure fails. As far as the applicability of this specific high-rise frame-core tube structure is concerned, its limit state threshold refers to the relevant regulations on story drift in the "Code for Seismic Design of Buildings" (GB 50011-2010). Specifically, Table 3 shows the limit state thresholds of story drift at different performance levels in the IDA-based seismic vulnerability analysis of high-rise frame-core tube structures. In this paper, the elastic-plastic story drift limit is set at $\theta_p = 1/100$.

4 Study on failure modes based on IDA method

4.1 Selection of ground motion

The selection of ground motion has a significant effect on the calculation results of IDA method for structural failure. According to the response spectrum stipulated in Code for Seismic Design of Buildings (GB 50011-2010) as the target spectrum, 15 ground motions were selected, and the peak ground acceleration (PGA) of ground motions was distributed over a broad intensity range, as shown in Table 4. The corresponding period of the selected ground motion is in good agreement with the main mode shape, and the shear force at the bottom of the structure is 70%–130% of the mode-superposition response spectrum method, and 80%–120% of the average value. The amplitude modulation method is utilized to modulate ground motion. The amplitude modulation step is 0.1 g, and the peak acceleration is 1.0 g.

4.2 Failure mode

4.2.1 Failure of isolated layer

The failure analysis of the isolated layer is divided into two parts: the base isolated layer and the upper isolated layer. The maximum horizontal displacement of the base isolated layer corresponds to the maximum horizontal displacement envelope value of the isolated layer at the base of the core tube, while the maximum horizontal displacement of the upper isolated layer corresponds to the maximum horizontal displacement envelope value of the isolated layer at the frame part. Under ground motion, the maximum surface pressure and minimum surface pressure of an isolated layer correspond to the minimum vertical stress and maximum vertical stress of all isolated bearings of the isolated layer, respectively. Figure 6 depicts IDA curves of horizontal displacement of base isolated layer and IDA curve of horizontal displacement of upper isolated layer. The end point of IDA curve of single ground motion is PGA when the horizontal displacement of isolated layer exceeds 385 mm. Figure 7 depicts the maximum and minimum vertical stresses of the base isolated layer, while Figure 8 depicts the maximum and minimum vertical stresses of the upper isolated layer. Positive stress is tensile stress, and the negative stress is compressive stress. The IDA curve representing the maximum vertical stress of an isolated layer caused by a single ground motion ends at the PGA corresponding to a vertical stress exceeding 1 MPa.

The allowable structural-load-carrying capability of rubber bearing decreases as horizontal shear deformation increases. The IDA curves reveal that the horizontal displacement of the upper isolated layer is typically greater than that of the base isolated layer, indicating that the upper isolated layer is subject to a greater horizontal shear force than the base isolated layer under ground motion and is therefore more susceptible to fail.

The calculation of vertical stress of isolated layer reveals that the upper isolated layer and the base isolated layer do not exceed

TABLE 4 Ground motions.

No.	Event name	Record seq.	Tg/g	Magnitude	Rjb(km)	Rrup(km)
GM1	Big Bear-01	909	0.53	6.46	77.33	78.21
GM2	Chalfant valley-02	549	0.38	6.19	14.38	17.17
GM3	Chi-Chi, Taiwan-04	2738	0.3	6.2	50.26	50.29
GM4	Gilroy	2033	0.31	4.9	29.63	30.66
GM5	Imperial valley-06	188	0.31	6.53	30.33	30.33
GM6	Landers	836	0.68	7.28	87.94	87.94
GM7	Livermore-01	216	0.36	5.8	53.35	53.82
GM8	Northridge-01	948	0.31	6.69	41.11	41.41
GM9	San Fernando	66	0.25	6.61	139.14	139.14
GM10	Superstition hills-01	718	0.43	6.22	17.59	17.59
GM11	Caldiran, Turkey	1627	0.2	7.21	50.78	50.82
GM12	Coalinga-03	393	0.58	5.38	12.77	13.32
GM13	Erzican, Turkey	821	0.52	6.69	0	4.38
GM14	Hector mine	1768	0.6	7.13	61.2	61.2
GM15	Kocaeli, Turkey	1165	0.37	7.51	3.62	7.21

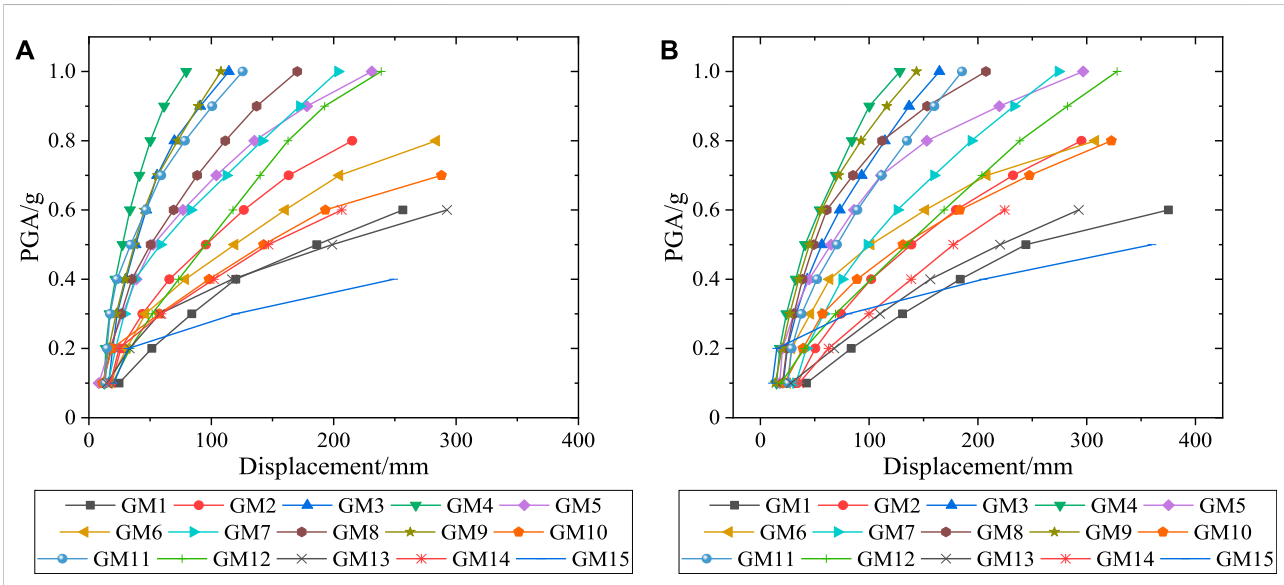

FIGURE 6
Horizon displacement of isolated layers: **(A)** Base isolated layer, **(B)** Upper isolated layer.

the vertical compressive stress limit of isolated bearing, and that the maximum compressive stress, 13.07 MPa, is located in the upper isolated layer. According to the IDA curves of the maximum vertical stress of the two isolated layers, the isolated bearings are consistently under pressure for the majority of ground motions. As the ground motion PGA increases, tensile stress will arise in some bearings of the isolated layer, and there is a risk of overturning and collapse of the structure. Comparing the IDA curve of maximum vertical stress of the base isolated layer and the upper isolated layer reveals that tensile stress and tensile

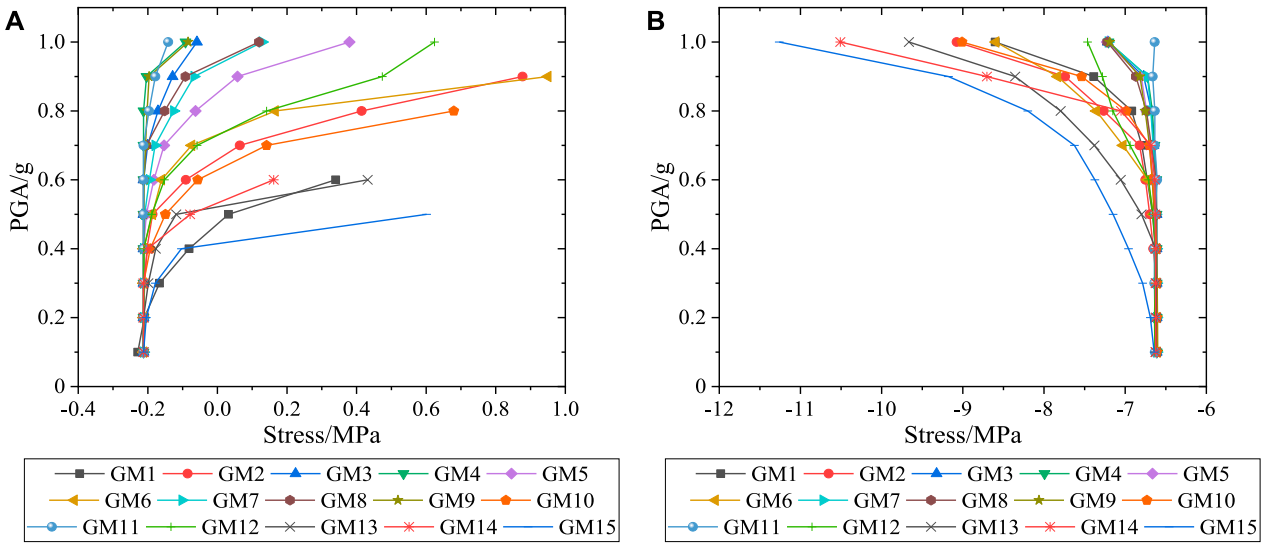

FIGURE 7
Base isolated layer: **(A)** Maximum vertical stress, **(B)** Minimum vertical stress.

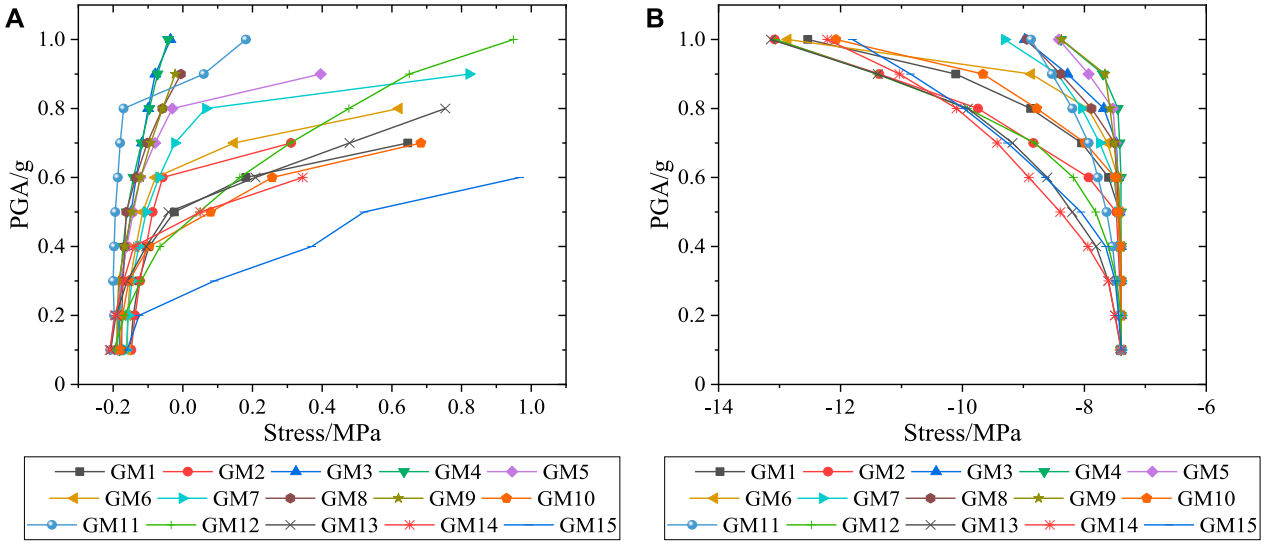

FIGURE 8
Upper isolated layer: **(A)** Maximum vertical stress, **(B)** Minimum vertical stress.

stress exceeding limit are more likely to occur in the upper isolated layer under the same ground motion, indicating that structural-load-carrying capacity failure of the upper isolated layer is more probable than that of the base isolated layer.

Through comprehensive comparison of IDA curve of horizontal displacement and the IDA curve of vertical stress of the isolated layers under different PGA ground motions of the new staggered story isolated structure, the upper isolated layer is more prone to failure than the base isolated layer. After the interlayer deformation of the structure due to ground motion, the upper isolated layer is no longer perpendicular to the direction of gravity, and the component force of gravity in the direction

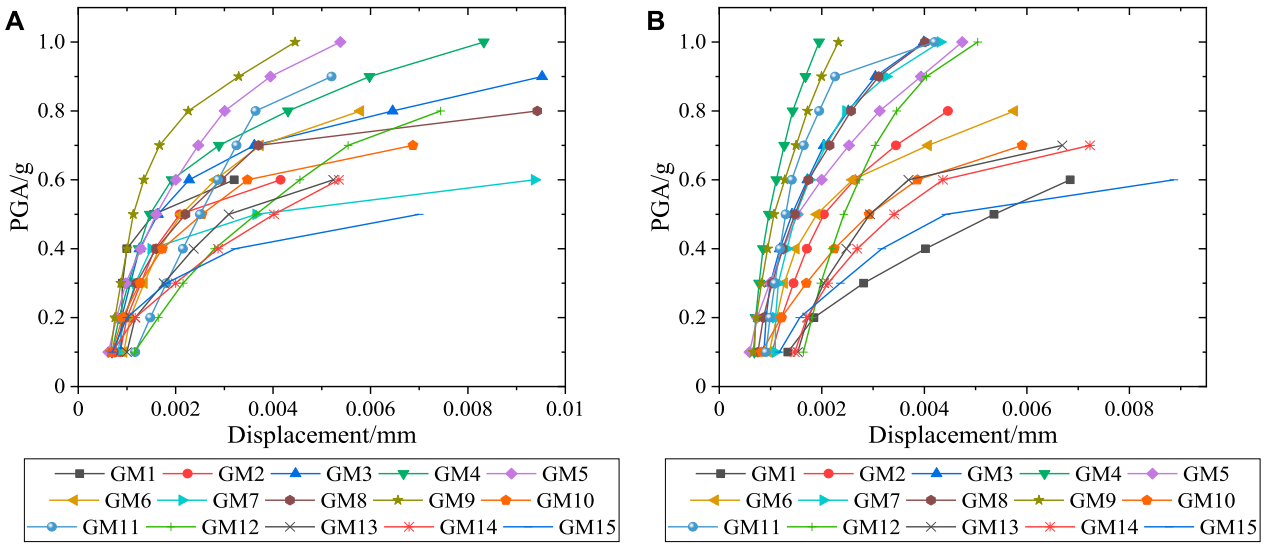

FIGURE 9
Maximum story drift of major structure: **(A)** Frame, **(B)** Core tube.

parallel to the floor slab acts as the lateral force of the floor under the influence of P-δ effect.

4.2.2 Failure of major structure

The core tube of the new staggered story isolated structure is separated from the frame below the upper isolated layer, whereas above the upper isolated layer they are connected by beams, therefore the primary structure's story drift is considerably different below the upper isolated layer. Using the IDA curve of maximum story drift of the core tube and the IDA curve of maximum story drift of the frame, the major failure modes of the new staggered structure are analyzed. Figure 9 depicts the IDA curves of the maximum horizontal story drift of a major structure. The IDA curve of the maximum story drift of the major structure caused by a single ground motion terminates at the corresponding PGA where the displacement angle exceeds 1/100.

The comparison of the IDA curves maximum story drift of the frame and the core tube indicates that the frame of the new staggered story isolated structure is more likely to be destroyed before the core tube under strong ground motion. Typically, the probability of the maximum story angle of the frame part appearing at the bottom layer is 61.3%, and the probability of appearing near the upper isolated layer is 14.6%. The probability of the maximum story angle of the core tube appearing at the bottom layer is 74% because the base isolated layer is set at the bottom of the core tube, which lessens the stiffness of the bottom of the core tube.

The major structure failure mode of the new staggered story isolated structure shows that the structural failure usually occurs at the bottom of the whole structure and the frame near the upper isolated layer. The new staggered story isolated structure has unique structural characteristics, that is, only the frame above the upper isolated layer is connected with the core tube, forming a structural characteristic similar to that of the inter-story isolated structure. Therefore, when seismic damage reaches the failure criterion of the core tube, the frame part connected above the upper isolated layer will also be damaged accordingly.

When a major structure fails, Table 5 displays the corresponding ground motion, PGA, horizontal displacement of isolated layers, maximum vertical stress, and minimum vertical stress of isolated layers. When the primary structure of the new staggered story isolated structure fails, the vertical stress and horizontal displacement of the isolated layer are typically still within the limit range. When the horizontal displacement of an isolated layer exceeds the limit, the tensile stress of isolated layer will also exceed the limit. Therefore, the failure of the major structure of the new staggered story isolated structure is prior to the failure of the isolated layer. Therefore, structural design should be given further consideration.

4.3 Weakest failure mode

As can be seen from the table of major structure failure, when the PGA of most ground motion hits 1.0 g, the major structure and isolated layer are severely deformed and damaged. When isolated layer failure and major structure failure occur under GM1, the PGA is at its minimal. Therefore, the failure mode under GM1 is the weakest failure mode.

TABLE 5 Failure of major structure.

Number	PGA/g	Horizontal displacement/mm		Vatical stress/MPa	
		Base isolated	Upper isolated	Minimum	Maximum
GM1	0.7	556	633	−8.044	1.051
GM2	0.7	163	232	−8.837	0.310
GM3	1.0	114	201	−8.976	−0.058
GM6	0.9	564	590	−8.871	2.037
GM7	0.7	112	159	−7.748	0.821
GM8	0.9	137	166	−8.390	−0.005
GM10	0.8	431	551	−8.779	1.219
GM11	1.0	125	185	−8.874	0.181
GM12	0.9	192	282	−11.405	0.652
GM13	0.7	489	514	−9.178	1.347
GM14	0.7	504	589	−9.432	1.245
GM15	0.6	620	694	−11.804	2.654

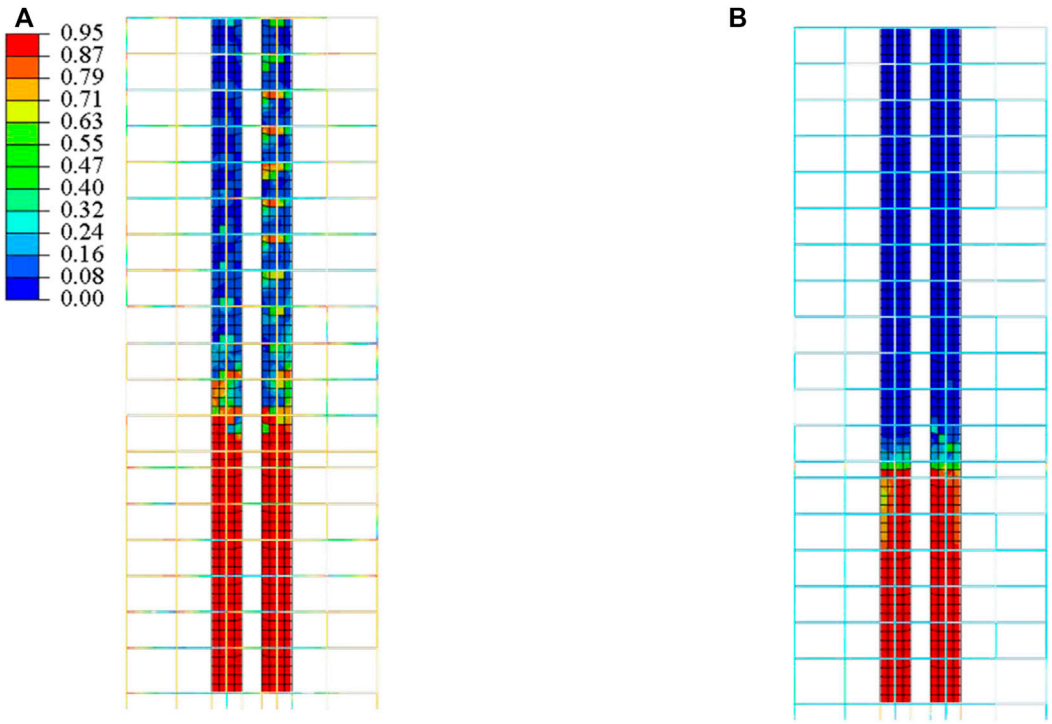

FIGURE 10
The damage of the new staggered story isolated structure: **(A)** Tensile damage, **(B)** Compressive damage.

Under GM1, the damage of the new staggered story isolated structure is shown in Figure 10. As seen in the diagram, the damage to structural components is concentrated in the area beneath the upper isolated layer of the structure. With an increase in ground motion PGA, the damage increases and the structural-load-carrying capacity lost, resulting in the

TABLE 6 Failure path.

Sequence	Number	Sequence	Number
1	1C20	16	6S41-42
2	2C20	17	6S39-40
3	2B19-20	18	7S41-42
4	2C12	19	7S39-40
5	2C11	20	I19
6	2S41-42	21	I20
7	2S39-40	22	I21
8	3C11	23	I24
9	3S41-42	24	I25
10	3S39-40	25	8B19-38
11	4S41-42	26	8B17-37
12	4S39-40		
13	5C10		
14	5S41-42		
15	5S39-40		

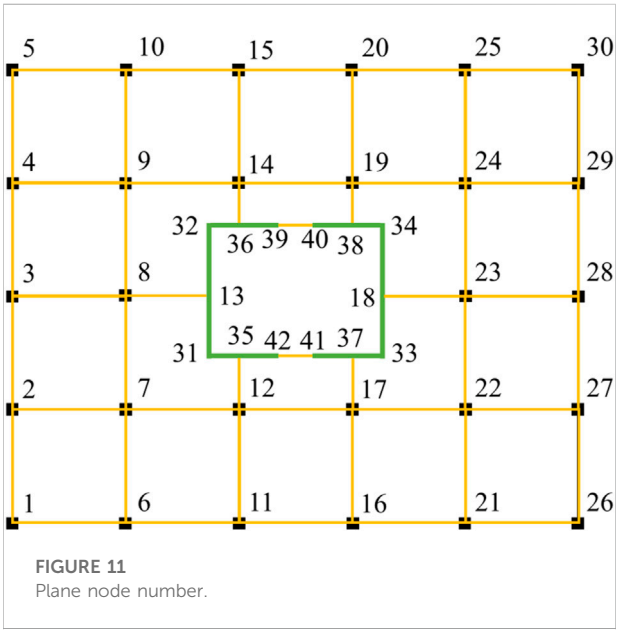

FIGURE 11
Plane node number.

collapse of the major structure. Table 6 depicts the failure path of this model for the new staggered story isolated structure under GM1. The failure of the isolated bearing is mainly due to the overrun of displacement and tension and compression stress. The failure mode of the isolated bearing in the damage path is mainly due to the overrun of the tensile stress. The first digit in the table represents the floor where the component is located. The second digit of the number is the type of the component: B represents the beam, C represents the column, I represents the isolated bearing, and S represents the shear wall. The third digit represents the plane position of the floor on which the member is located, which can be confirmed by the plane node number of the column component and shear wall component, as shown in Figure 11. For instance, column No. 20 on the first floor is designated as 1C20, while the beam between column No. 20 and column No. 15 on the second floor is designated as 2B15-20.

5 Further research

In this paper, IDA method is used to identify the failure mode of the new staggered story isolated structure. Based on this, further research can be carried out in the following aspects:

1) According to the analysis of the failure mode of the new staggered story isolated structure, the optimization of the structure can be divided into two categories: major structure optimization and isolated layer optimization. According to the optimization of the failure mode of the inter-story structure, selecting materials with greater strength for the major structure can effectively optimize and reduce the failure probability of the structure (Dezfuli and Alam, 2013; Jin et al., 2020).
2) The insufficient supporting capacity of the frame beneath the upper isolated layer is identified as the primary cause of the failure of the major structure. Therefore, raising the upper isolated layer area of the new staggered story isolated structure is greatly beneficial to the bearing capacity and collapse resistance of the structure. For instance, a large chassis frame structure is designed below the upper isolated layer to expand the area of the upper isolated layer, making the structure more inclined to the layer isolated structure and ensuring the stability of the lower structure (Charmpis et al., 2012; Zhang et al., 2021).
3) In this paper, the failure modes of the new staggered story isolated structure are analyzed but the failure modes of the inter-story isolated structure and the base isolated structure are not compared. The new staggered story isolated structure is a new type of isolated structure developed based on inter-story and base isolated structures. Whether its failure probability is better than other isolated structures in the face of large earthquakes remains to be studied and verified.

6 Conclusion

In this paper, a new staggered story isolated structure model was established, and the failure mode of the new staggered story isolated structure was identified by using the IDA method based on the failure criteria of the major structure and the isolated layer.

By analyzing the failure mode of the major structure of the new staggered story isolated structure, the failure mode of the isolated layer, the weakest failure mode and the corresponding damage and failure paths, the following conclusions are drawn:

1) The new staggered story isolated structure has a high collapse resistance and the structure can maintain good structural performance under most of the ground motion.
2) The unique double isolated layer ensures the integrity of the core cylinder and dampens structural response. It is found that the upper isolated layer is prone to internal tensile stress under the influence of the P-δ effect, resulting in the failure of the isolated layer. Below the upper isolated layer, the frame part of the structure is separated from the core tube part, rendering the core tube incapable of restricting the displacement of the frame, hence increasing the likelihood that the frame part below the isolated layer will fail.
3) Comparing the horizontal displacements of isolated layers, the displacement of the upper isolated layer is greater than that of the base isolated layer, indicating a greater probability of failure. The tensile stress of the upper isolated layer may exceed the limit, and there is a risk of the structure overturning under severe strong ground motions.
4) The failure of the structure is concentrated in the bottom and upper isolated layer of the structure, with multiple weak positions of the upper isolated layer. In the structural design, the weak point of the structure should be strengthened.
5) For the failure modes of the new staggered story isolated structure, two distinct optimization modes are proposed. Increase the thickness of the core tube shear wall beneath the upper isolated layer and focus on improving the cross-section size of the bottom frame beam column, and improve the bearing capacity of the structure. Increasing the area of the upper isolated layer can effectively enhance the collapse resistance and stability of the structure.

Data availability statement

The raw data supporting the conclusions of this article will be made available by the authors, without undue reservation.

Author contributions

LC; Conceptualization, Methodology, Software, Writing; TW: Data curation; QW: Data curation; DL:Visualization, Supervision; ZX: Writing-Reviewing and Editing; GL: Software ZY: Software ML: Writing-Reviewing and Editing.

Conflict of interest

The authors declare that the research was conducted in the absence of any commercial or financial relationships that could be construed as a potential conflict of interest.

Publisher's note

All claims expressed in this article are solely those of the authors and do not necessarily represent those of their affiliated organizations, or those of the publisher, the editors and the reviewers. Any product that may be evaluated in this article, or claim that may be made by its manufacturer, is not guaranteed or endorsed by the publisher.

References

Ahmadi, H. R., Mahdavi, N., and Bayat, M. (2020). Applying adaptive pushover analysis to estimate incremental dynamic analysis curve. *J. Earthq. Tsunami* 14, 2050016. doi:10.1142/s1793431120500165

Becker, T. C., Yamamoto, S., Hamaguchi, H., Higashino, M., and Nakashima, M. (2015). Application of isolation to high-rise buildings: A Japanese design case study through a US design code lens. *Earthq. Spectra* 31, 1451–1470. doi:10.1193/052813eqs136m

Castaldo, P., Palazzo, B., and Della Vecchia, P. (2015). Seismic reliability of base-isolated structures with friction pendulum bearings. *Eng. Struct.* 95, 80–93. doi:10.1016/j.engstruct.2015.03.053

Castaldo, P., and Tubaldi, E. (2018). Influence of ground motion characteristics on the optimal single concave sliding bearing properties for base-isolated structures. *Soil Dyn. Earthq. Eng.* 104, 346–364. doi:10.1016/j.soildyn.2017.09.025

Chang, P. J., and Zhu, J. (2011). Seismic vulnerability analysis of mid-story isolation and reduction structures based stochastic vibration. *Adv. Mater. Res.* 243, 3988–3991. doi:10.4028/www.scientific.net/amr.243-249.3988

Charmpis, D. C., Komodromos, P., and Phocas, M. C. (2012). Optimized earthquake response of multi-storey buildings with seismic isolation at various elevations. *Earthq. Eng. Struct. Dyn.* 41, 2289–2310. doi:10.1002/eqe.2187

Derham, C. J., Kelly, J. M., and Thomas, A. G. (1985). Nonlinear natural rubber bearings for seismic isolation. *Nucl. Eng. Des.* 3, 417–428. doi:10.1016/0029-5493(85)90258-4

Dezfuli, F. H., and Alam, M. S. (2013). Multi-criteria optimization and seismic performance assessment of carbon FRP-based elastomeric isolator. *Eng. Struct.* 49, 525–540. doi:10.1016/j.engstruct.2012.10.028

Du, Y., Duan, H., and Xu, T. (2018). Vertical progressive collage mechanism and influencing factors of base-isolated structures. *J. Vib. Shock* 37, 257–264.

Faiella, D., and Mele, E. (2020). Insights into inter-story isolation design through the analysis of two case studies. *Eng. Struct.* 215, 110660. doi:10.1016/j.engstruct.2020.110660

Franke, S., Franke, B., and Harte, A. M. (2015). Failure modes and reinforcement techniques for timber beams – state of the art. *Constr. Build. Mater.* 97, 2–13. doi:10.1016/j.conbuildmat.2015.06.021

Güneş, N., and Ulucan, Z. Ç. (2021). Collapse probability of code-based design of a seismically isolated reinforced concrete building. *Structures* 33, 2402–2412. doi:10.1016/j.istruc.2021.06.010

Haiyang, Z., Xu, Y., Chao, Z., and Dandan, J. (2014). Shaking table tests for the seismic response of a base-isolated structure with the SSI effect. *Soil Dyn. Earthq. Eng.* 67, 208–218. doi:10.1016/j.soildyn.2014.09.013

He, X., and Lu, Z. (2019). Seismic fragility assessment of a super tall building with hybrid control strategy using IDA method. *Soil Dyn. Earthq. Eng.* 123, 278–291. doi:10.1016/j.soildyn.2019.05.003

Huan, J., Ma, D., and Wang, W. (2018). Vulnerability analysis of ancient timber architecture by considering the correlation of different failure modes. *Math. Problems Eng.* 2018, 1–10. doi:10.1155/2018/5163472

Jin, J., Xiao, J., Tan, P., Liu, Y., and Huang, X. (2020). Study on failure modes of base-isolated structures based on IDA method. *J. Seismol. Res.* 43, 463–470.

Kelly, J. M. (1990). Base isolation; linear theory and design. *Earthq. Spectra* 6, 223–244. doi:10.1193/1.1585566

Kim, H. S., and Kang, J. W. (2018). Vibration control performance evaluation of hybrid mid-story isolation system for a tall building. *J. korean Assoc. For Spatial Struct.* 18, 37–44. doi:10.9712/kass.2018.18.3.37

Kim, H. S., Kim, S. G., and Kang, J. W. (2018). Seismic response evaluation of mid-story isolation system according to the change of characteristics of the seismic isolation device. *J. korean Assoc. For Spatial Struct.* 18, 109–116. doi:10.9712/kass.2018.18.1.109

Kitayama, S., and Constantinou, M. C. (2019). Effect of displacement restraint on the collapse performance of seismically isolated buildings. *Bull. Earthq. Eng.* 17, 2767–2786. doi:10.1007/s10518-019-00554-y

Liu, D., Li, L., Zhang, Y., Chen, L., Wan, F., and Yang, F. (2022). Study on seismic response of a new staggered story isolated structure considering ssi effect. *J. Civ. Eng. Manag.* 28, 397–407. doi:10.3846/jcem.2022.16825

Loh, C., Weng, J., Chen, C., and Lu, K. C. (2013). System identification of mid-story isolation building using both ambient and earthquake response data. *Struct. Control Health Monit.* 20, 139–155. doi:10.1002/stc.479

Ministry of Housing and Urban-Rural Development (2010). *Code for design of concrete structures: GB 50010-2010*. Beijing, China: China Architecture and Building Press.

Ministry of Housing and Urban-Rural Development (2010). *Code for seismic design of buildings: GB 50011-2010*. Beijing, China: China Architecture and Building Press.

Ministry of Housing and Urban-Rural Development (2010). *Technical specification for concrete structures of Tall buildings: Jgj 3 – 2010*. Beijing, China: China Architecture and Building Press.

Navideh, M., Hamid, R. A., and Hamed, M. (2012). A comparative study on conventional push-over analysis method and incremental dynamic analysis (IDA) approach. *Sci. Res. essays* 7, 751–773. doi:10.5897/SRE10.042

Nazarnezhad, T., and Naderpour, H. (2021). Probabilistic damage evaluation of base-isolated reinforced concrete structures under near-fault pulse-like bidirectional seismic excitations. *Structures* 32, 1156–1170.

Pan, Y., Bao, Y., Liu, Y., and Hu, S. (2021). Seismic fragility analysis of base-isolation structure connected with large span special-shaped steel corridor. *China Civ. Eng. J.* 54, 20–29.

Pant, D. R., and Wijeyewickrema, A. C. (2012). Structural performance of a base-isolated reinforced concrete building subjected to seismic pounding. *Earthq. Eng. Struct. Dyn.* 41, 1709–1716. doi:10.1002/eqe.2158

Shafigh, A., Ahmadi, H. R., and Bayat, M. (2021). Seismic investigation of cyclic pushover method for regular reinforced concrete bridge. *Struct. Eng. Mech. Int'l J.* 78, 41–52.

Shan, J., Shi, Z., Gong, N., and Shi, W. (2020). Performance improvement of base isolation systems by incorporating eddy current damping and magnetic spring under earthquakes. *Struct. Control Health Monit.* 27, 2524. doi:10.1002/stc.2524

Shi, C., and Du, Y. (2021). Evaluation of the collapse mode of isolated structures subjected to multi-directional dynamic coupling excitation based on reliability theory. *Structures* 34, 1261–1275. doi:10.1016/j.istruc.2021.08.037

Song, L., Fei, C., Wen, J., and Bai, G. C. (2017). Multi-objective reliability-based design optimization approach of complex structure with multi-failure modes. *Aerosp. Sci. Technol.* 64, 52–62. doi:10.1016/j.ast.2017.01.018

Sueoka, T., Torii, S., and Tsuneki, Y. (2004). "The application of response control design using middle-story isolation system to high-rise building," in 13th World Conference on Earthquake Engineering Vancouver, Canada, August 1-6, 2004.

Tan, P., Huang, J., Chang, C., and Zhang, Y. (2017). Failure modes of a seismically isolated continuous girder bridge. *Eng. Fail. Anal.* 80, 57–78. doi:10.1016/j.engfailanal.2017.05.030

Tan, Y., Zhu, B., Qi, L., Yan, T., Wan, T., and Yang, W. (2020). Mechanical behavior and failure mode of steel–concrete connection joints in a hybrid truss bridge: Experimental investigation. *Materials* 13, 2549. doi:10.3390/ma13112549

Tavakoli, H. R., Naghavi, F., and Goltabar, A. R. (2015). Effect of base isolation systems on increasing the resistance of structures subjected to progressive collapse. *Earthquakes Struct.* 9, 639–656. doi:10.12989/eas.2015.9.3.639

Tsuneki, Y., Torii, S., Murakami, K., and Sueoka, T. (2008). "Middle-story isolated structural system of high-rise building," in The 14 th World Conference on Earthquake Engineering, Beijing, China, October 12-17, 2008.

Wang, S., Chang, K., Hwang, J., Hsiao, J. Y., Lee, B. H., and Hung, Y. C. (2012). Dynamic behavior of a building structure tested with base and mid-story isolation systems. *Eng. Struct.* 42, 420–433. doi:10.1016/j.engstruct.2012.04.035

Whittaker, A. S., Sollogoub, P., and Kim, M. K. (2018). Seismic isolation of nuclear power plants: Past, present and future. *Nucl. Eng. Des.* 338, 290–299. doi:10.1016/j.nucengdes.2018.07.025

Yan, X., and Xu, L. (2018). Multi-objective optimization of genetic algorithm-based failure mode for reinforced concrete frame-shear wall structures. *Eng. Mech.* 35, 69–77.

Ye, K., Li, L., and Zhu, H. (2009). A modified Kelvin impact model for pounding simulation of base-isolated building with adjacent structures. *Earthq. Eng. Eng. Vib.* 8, 433–446. doi:10.1007/s11803-009-8045-4

Zhang, H., Li, F., Tai, J., and Zhou, J. (2021). Research on structural design of an isolated high-rise building with enlarged base and multiple tower layer in high-intensity area. *Math. Problems Eng.* 2021, 1–14. doi:10.1155/2021/6669388

Zhang, Y., Liu, D., Fang, S., Lei, M., Zhu, Z., and Liao, W. (2022). Study on shock absorption performance and damage of a new staggered story isolated system. *Adv. Struct. Eng.* 25, 1136–1147. doi:10.1177/13694332211056113

Zhang, Y., Tan, P., and Huang, J. (2018). Failure mode of isolated beam bridge by weighted rank sum ratio method. *J. Southwest Jiaot. Univ.* 53, 72–78.

Zhao, Z., Dai, K., Camara, A., Bitsuamlak, G., and Sheng, C. (2019). Wind turbine tower failure modes under seismic and wind loads. *J. Perform. Constr. Facil.* 2, 0001279. doi:10.1061/(asce)cf.1943-5509.0001279

Zheng, S., Yang, W., Yang, F., Sun, L., and Hou, P. (2015). Seismic fragility analysis for RC core walls structure based on IDA method. *J. Vib. Shock* 34, 117–123.

Zhou, Q., Singh, M. P., and Huang, X. Y. (2016). Model reduction and optimal parameters of mid-story isolation systems. *Eng. Struct.* 124, 36–48. doi:10.1016/j.engstruct.2016.06.011

Zhou, Y., Li, X., and Chen, Z. (2018). *Seismic responses analysis of base-isolated LNG storage tank*. Singapore: Springer Singapore, 331–339.

Zhou, Y., Su, N., and Lu, X. (2013). Study on intensity measure of incremental dynamic analysis for high-rise structures. *J. Build. Struct.* 34, 53–60.